CHAPTER 4

Results

4.1 Characteristics of the Targets

From the previous chapter, the characteristics of our targets eg. B, V, R, T-$Type$ and $EW(\mathrm{H}\alpha)$ were already determined. The value of the parameters and the images of some samples are shown in Tables 4.1 and A.3, respectively. The correlation between the parameters to understand the stellar content of the galaxies were examined.

4.2 Color Indices and B_{25} Magnitude

Result shows that color indices of our sample vary in range: $0.6 - 1.0$ for $B-V$, $0.9 - 1.4$ for $B-R$ and $0.2 - 0.4$ for $V-R$. M_B magnitude scatters in a wide range, from -21 to -15 magnitude, without correlation with the color indices as shown in Figure 4.1.

4 out of 5 bright galaxies (magnitude brighter than -20.0 in B, brighter than -21 in V and R) are elliptical galaxies with T-$Type$ of -5 and the other one is a spiral galaxy with T-$Type$ of 1. Moreover, bright elliptical galaxies tend to become bluer as it becomes brighter. This is also observed with fainter elliptical galaxies of magnitudes fainter than -19.0.

ลิขสิทธิ์มหาวิทยาลัยเชียงใหม่
Copyright© by Chiang Mai University
All rights reserved

Table 4.1: The parameters of the galaxies in NGC 4065 group

No.	Name	B	V	R	$B-V$	$B-R$	$V-R$	*T-Type*	$EW(\mathrm{H}\alpha)$	S/N
1	NGC 4070	-20.90	-21.79	-22.10	0.89	1.20	0.31	-5	3.504	2.6
2	J12040831+2023280	-17.95	-18.83	-19.11	0.88	1.16	0.28	-5	-0.075	-0.1
3	NGC 4066	-20.90	-21.78	-22.06	0.88	1.16	0.28	-5	6.359	2.4
4	NGC 4069	-18.03	-18.99	-19.40	0.96	1.37	0.41	-5	9.928	3.2
5	NGC 4060	-19.00	-19.83	-20.07	0.83	1.07	0.24	-2	13.915	4.4
6	NGC 4056	-17.80	-18.66	-19.03	0.86	1.23	0.37	-5	-0.803	-0.3
7	NGC 4065	-20.45	-21.40	-21.80	0.95	1.35	0.40	-5	5.005	2.4
8	J12040495+2014489	-17.80	-18.74	-19.16	0.94	1.36	0.42	-5	2.522	1.4
9	NGC 4061 (4055)	-20.29	-21.26	-21.69	0.97	1.40	0.43	-5	5.392	3.0
10	NGC 4072	-18.69	-19.68	-20.08	0.99	1.39	0.40	-2	6.950	4.4
11	UGC 07049	-18.44	-19.23	-19.56	0.79	1.12	0.33	5	27.053	18.5
12	J12041217+2010251	-17.21	-18.18	-18.54	0.97	1.33	0.36	-2	0.375	0.2
13	NRGb177.059	-15.88	-16.79	-17.28	0.91	1.40	0.49	4	18.157	18.2
14	J12043987+2013411	-18.11	-19.07	-19.53	0.96	1.42	0.46	-2	2.460	4.2
15	NGC 4076	-20.20	-20.89	-21.27	0.69	1.07	0.38	1	12.789	19.0
16	J120425.68+201548.9	-16.36	-17.20	-17.46	0.84	1.10	0.26	-5	-6.699	-2.1
17	12042275+2015271	-17.28	-18.19	-18.48	0.91	1.20	0.29	-5	0.543	0.2
18	J12035600+2025499	-17.95	-18.93	-19.34	0.98	1.39	0.41	-2	3.234	5.3
19	J12034825+2024589	-17.91	-18.56	-18.84	0.65	0.93	0.28	5	10.835	16.1
20	J12035132+2003099	-18.83	-19.60	-19.76	0.77	0.93	0.16	3	13.168	4.9
21	J12032530+2014294	-18.35	-19.09	-19.29	0.74	0.94	0.20	-2	11.450	4.6

ลิขสิทธิ์มหาวิทยาลัยเชียงใหม่
Copyright© by Chiang Mai University
All rights reserved

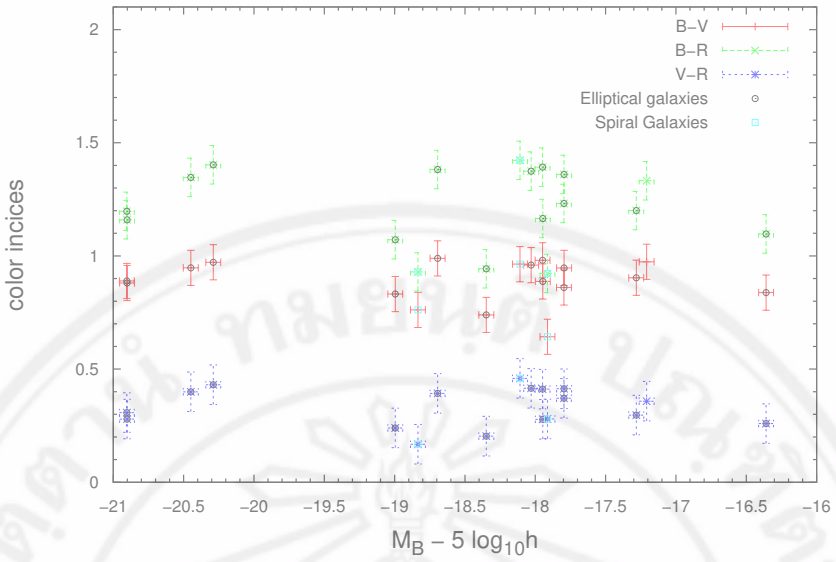

Figure 4.1: Plot between color indices and absolute magnitude M_B: red, green and blue dots represent $B-V$, $B-R$ and $V-R$ color indices, respectively.

Figures 4.2 and 4.3 show similar result for the plot against M_V and M_R. M_V and M_R magnitudes scatter in a wide range, from -22 to -16 and -22.5 to -17, respectively. Both brighter and fainter elliptical galaxies are acting the same as previous plot.

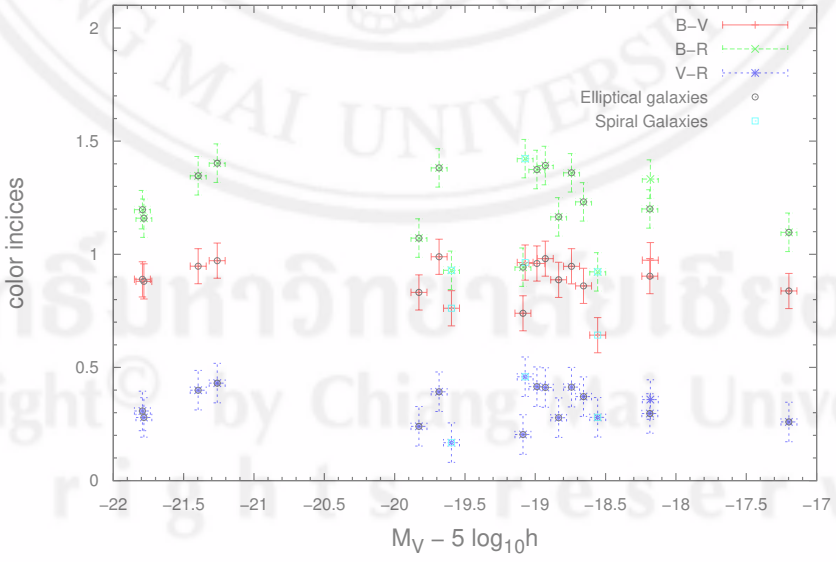

Figure 4.2: The plot between color indices and absolute magnitude M_V

ลิขสิทธิ์มหาวิทยาลัยเชียงใหม่
Copyright© by Chiang Mai University
All rights reserved

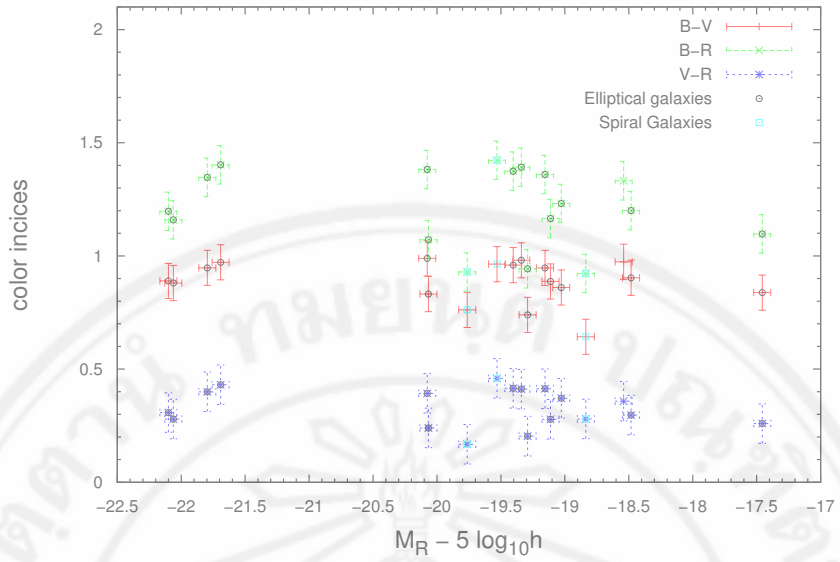

Figure 4.3: The plot between color indices and absolute magnitude M_R

4.3 Color Indices and T-$Type$

In this study, type of galaxies is separated into two groups, LTGs and ETGs. Their types are assigned according to the De Vaucoulers T-Type system: $T\text{-}Type \geq 0$ for LTGs and $T\text{-}Type < 0$ for ETGs. The plot between the color indices and the T-$Type$ shows us the difference between ETGs and LTGs.

ลิขสิทธิ์มหาวิทยาลัยเชียงใหม่
Copyright© by Chiang Mai University
All rights reserved

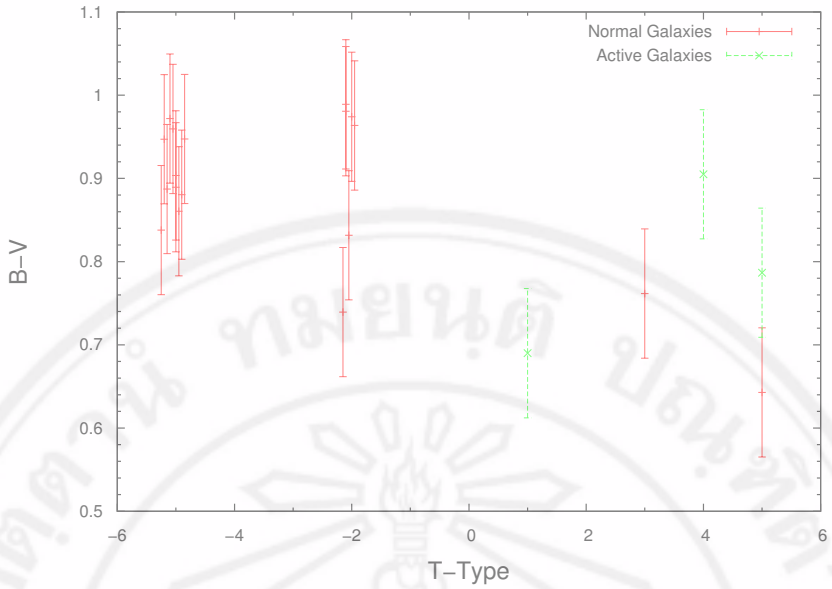

Figure 4.4: The plot between $B-V$ color and *T-Type*. The red cross are represent to the normal galaxies and the green one are active galaxies.

Figures 4.4, 4.5, and 4.6 exhibit the same behavior: the LTGs are bluer than ETGs. However, the range of their color indices varies as summarized in Table 4.2. This is consistent with the previous study by Iskra et al. [2001]. They observed the bright early and late type of galaxies for more than 140,000 objects in Sloan Digital Sky Survey (SDSS) database and found that there is a significant difference in color between the early and the late type galaxies along *T-Type*.

ลิขสิทธิ์มหาวิทยาลัยเชียงใหม่
Copyright© by Chiang Mai University
All rights reserved

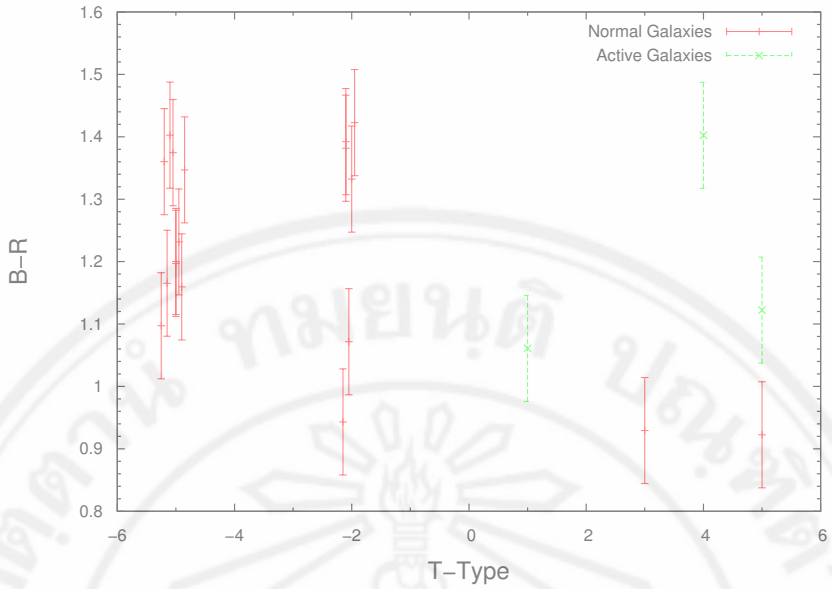

Figure 4.5: The plot between $B-R$ color and T-$Type$ with blue dots for the active galaxies

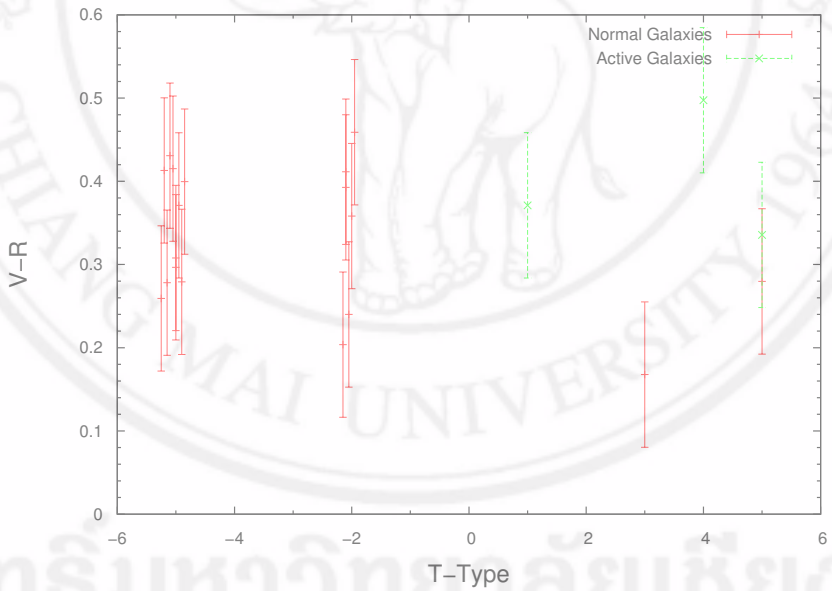

Figure 4.6: The plot between $V-R$ color and T-$Type$ with green dots for the active galaxies

ลิขสิทธิ์มหาวิทยาลัยเชียงใหม่
Copyright © by Chiang Mai University
All rights reserved

Table 4.2: Color Index Variations of the galaxies in NGC 4065 group in B, V and R_C filters

Color	ETGs	LTGs
$B-V$	0.75 - 1.00	0.65 - 0.75
$B-R$	0.95 - 1.50	0.90 - 0.95
$V-R$	0.20 - 0.45	0.15 - 0.30

4.4 Color Indices and $EW(\mathrm{H}\alpha)$

In this section, the galaxies are classified into normal galaxies and active galaxies. An active galaxy is a galaxy that has an active nucleus, called AG, at the center, making it much brighter than a normal galaxy. The luminosity from the nucleus can be more than the rest of the galaxy part itself. The active galaxies have a different star formation mechanism from normal galaxies, thus exhibiting a different trend from normal galaxies and the S/N < 3 galaxies.

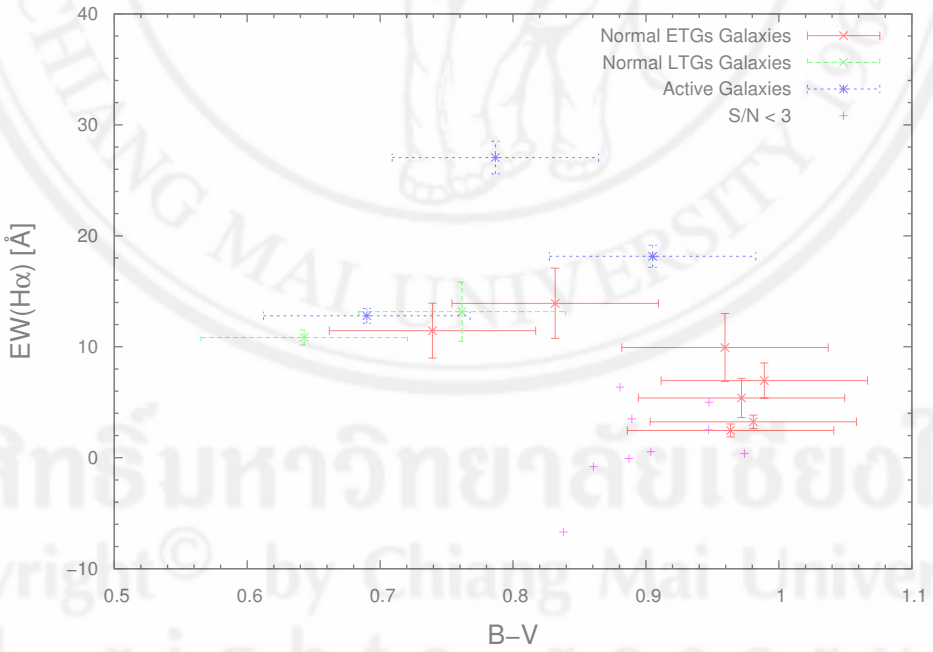

Figure 4.7: The plot between $EW(\mathrm{H}\alpha)$ and $B-V$ color.

From figure 4.7, the plot shows a diagram of $EW(\mathrm{H}\alpha)$ and $B-V$ color. After excluding three active galaxies and nine insignificant S/N galaxies, it was observed that

ลิขสิทธิ์มหาวิทยาลัยเชียงใหม่
Copyright© by Chiang Mai University
All rights reserved

for emission line galaxies, the bluer galaxies tend to have higher $EW(\mathrm{H}\alpha)$ than the redder one, and both normal LTGs galaxies have $EW(\mathrm{H}\alpha)$ than the most of the normal ETGs. All LTGs, including 3 active galaxies and blue ETGs with $B-V$ less than 0.85, have ongoing high star formation with $EW(\mathrm{H}\alpha) > 10$Å.

We also found the same result in Figures 4.8 and 4.9. The plot between $EW(\mathrm{H}\alpha)$ versus $B-R$ and $V-R$ color show that the bluer galaxies tend to have higher $EW(\mathrm{H}\alpha)$ than the redder galaxies. All LTGs, including 3 active galaxies and blue ETGs with $B-R$ less than 1.1 and $V-R$ less than 0.3, have ongoing high star formation with $EW(\mathrm{H}\alpha) > 10$ Å.

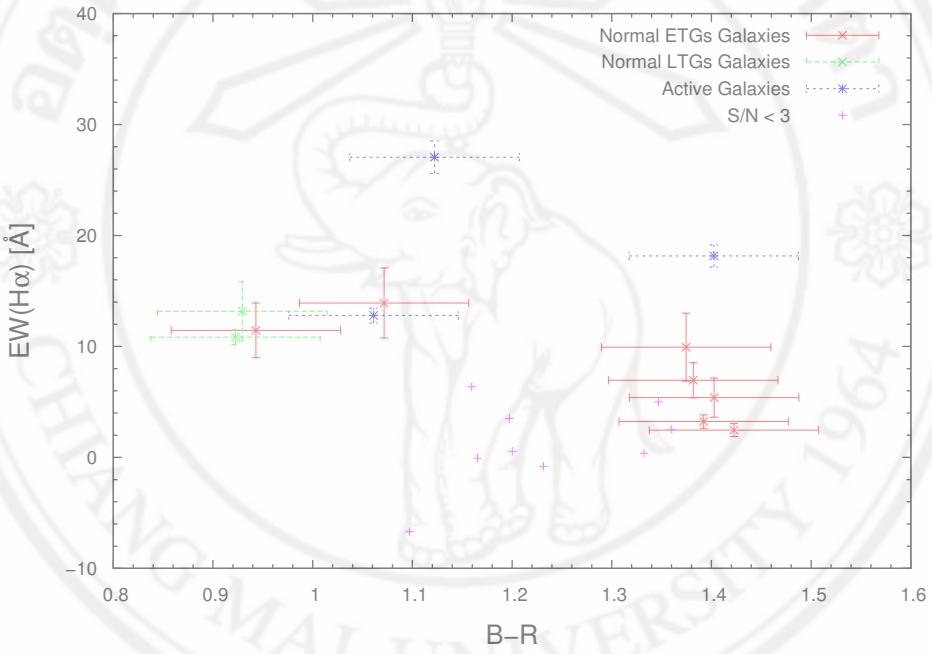

Figure 4.8: The plot between $EW(\mathrm{H}\alpha)$ and $B-R$ color.

From the plots between $EW(\mathrm{H}\alpha)$ and color indices, it can be inferred that all plots exhibit the same trend. Bluer galaxies tend to have more star formation activities than redder galaxies with $EW(\mathrm{H}\alpha)$ rate more than 10 Å when we exclude the AGN and S/N < 3 galaxies.

4.5 $EW(\mathrm{H}\alpha)$ and *T-Type*

The plot between $EW(\mathrm{H}\alpha)$ and *T-Type* in Figure 4.10 shows that the LTGs tend to have more $EW(\mathrm{H}\alpha)$ than the ETGs in normal group galaxies. One of the active galaxies

ลิขสิทธิ์มหาวิทยาลัยเชียงใหม่
Copyright© by Chiang Mai University
All rights reserved

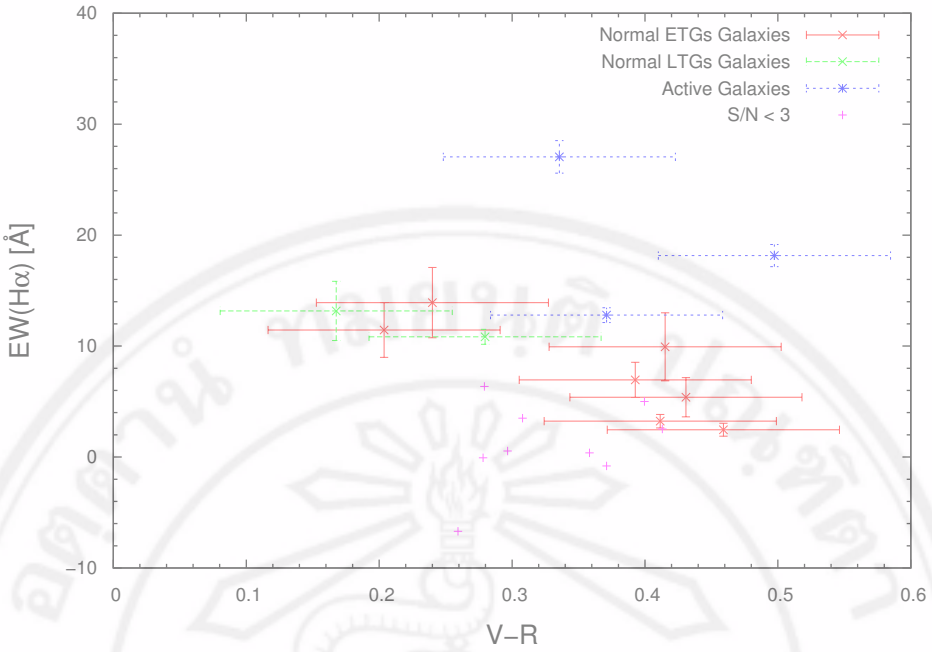

Figure 4.9: The plot between $EW(\mathrm{H}\alpha)$ and $V-R$ color.

exhibits the highest star formation activity. All late type and two S0 type galaxies show high star formation with $EW(\mathrm{H}\alpha) > 10$ Å, whereas the other early type sample was found to have $EW(\mathrm{H}\alpha)$, scattered between 5 - 15 Å. When results from previous study [Tasuya, 2012] were combined, it was observed that the galaxies in the NGC 4065 galaxy group act differently from the field galaxies.

4.6 Ongoing Star Formation in UGC07049

Investigating further into the area of the galaxies in our group that have high $EW(\mathrm{H}\alpha)$ or ongoing star formation to quantify some interaction parameters, it was observed that UGC07049 is the most star-forming galaxy in our sample which shows 27.05 ± 1.46 Å of $EW(\mathrm{H}\alpha)$ and is classified into LTGs Sc peculiar morphological type. This object has been well-studied by Freeland et al. [2010] via the 20-cm radio continuum emission. By using "HI deficiency" equation in Eq. 4.1, the predicted model is obtained from Haynes and Giovanelli [1984]. By using this predicted model with his observation parameters, they found that HI deficiency in UGC07049 is 0.41, 2.6 times more deficient than the normal HI region.

ลิขสิทธิ์มหาวิทยาลัยเชียงใหม่
Copyright© by Chiang Mai University
All rights reserved

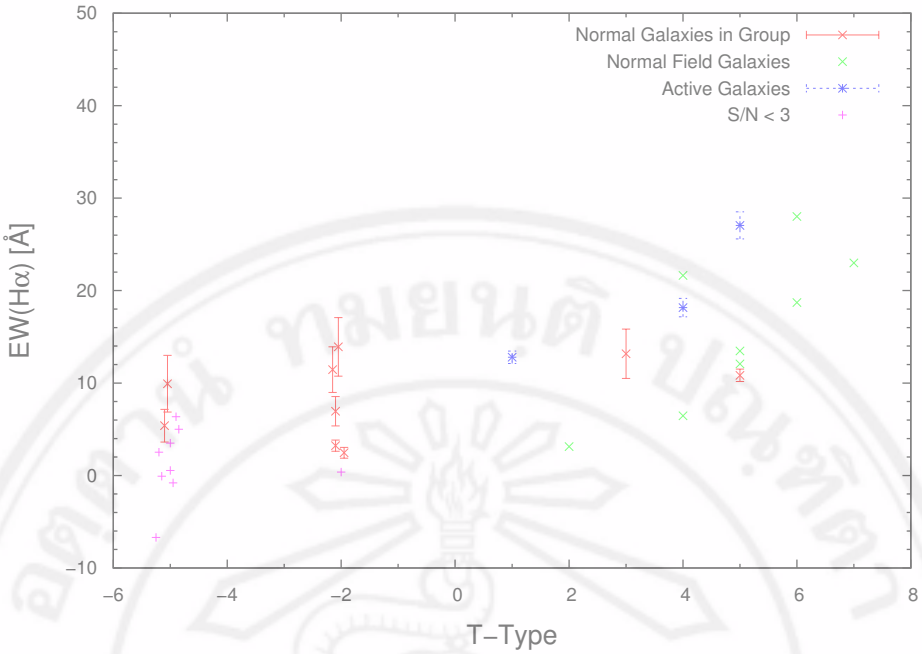

Figure 4.10: The plot between $EW(\mathrm{H}\alpha)$ and $T\text{-}Type$: small dots represent galaxies with S/N of $EW(\mathrm{H}\alpha) < 3$, whereas the others are emission line galaxies and field galaxies.

$$def_{HI} = \langle log\frac{M_{HI}}{D_i^2}\rangle_{predicted} - \langle log\frac{M_{HI}}{D_i^2}\rangle_{observed} \tag{4.1}$$

where

M_{HI} is the total HI mass of the galaxy, and

D_I is the B_{25} diameter (kpc).

From literature review in Chapter 2, there are two possible interactions causing HI deficiency: the tidal interaction between the galaxy and the cluster potential well, and the ram pressure stripping. By using the mass to light ratio model by Bell and de Jong [2001], $log(\frac{M}{L_B}) = 0.36$, it can be quantified that $M_{gal} = 8.65 \times 10^9$ $\mathrm{M_{sun}}$. The group velocity of NGC 4065 group is 6995 ± 48 km s^{-1} with a group velocity dispersion (σ) of 416 ± 35 km s^{-1} as surveyed by Mahdavi and Geller [2004]. The mass of the cluster is then calculated which is equal to $M_{cluster} = 8.77 \times 10^{13}$ $\mathrm{M_{sun}}$. The average perturbation of galaxy-cluster parameter, equal to $P_{gc} = 0.28$, can be calculated by using Eq. 2.5. This perturbation parameter only is not enough to cause that HI deficiency much [Byrd and

ลิขสิทธิ์มหาวิทยาลัยเชียงใหม่
Copyright© by Chiang Mai University
All rights reserved

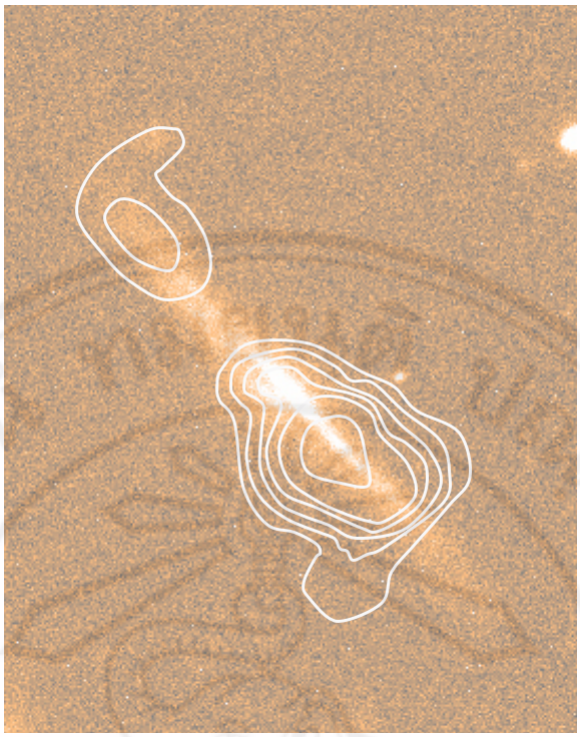

Figure 4.11: The image of UGC07049 in R band: white lines are the contours of HI density observed by Freeland et al. (2010) with the level of $(8.3, 24.9, 41.5, 58.1, 74.7, 91.3, 124.5, 166.0)$ x10^{19}.

Valtonen, 1990], leaving only the ram pressure stripping, tidal interaction and viscous stripping to remove the HI gas from this galaxy. The high $EW(\mathrm{H}\alpha)$ of this galaxy is resulted by active galaxy which is observed to be a radio galaxy by Jaffe et al. [1986].

4.7 Tidal Interaction Approximation

By using the mass-to-light ratio versus $B-R$ following TULLY-FISHER relation in Figure 4.12 (left) [Bell and de Jong, 2001], the mass of each galaxy is determined in units of solar mass. In this study, the average mass of the galaxaies in this group is 2.38×10^{10} $\mathrm{M_{Sun}}$.

Assuming that the group is virialized and uniformly spherical in shape, I used the virial theorem to derive the approximation of the mass of the NGC 4065 group following Eq. 4.2. From previous study, the radius of NGC 4056 group was calculated to be at 15 arc-minute (437 kpc at the distance of 100 Mpc) and the radial velocity dispersion (σ)

ลิขสิทธิ์มหาวิทยาลัยเชียงใหม่
Copyright© by Chiang Mai University
All rights reserved

which equal to 416 ± 35 km.s^{-1} [Helsdon and Ponman, 2000]. These values can be use to determine the mass of the group. The mass of the NGC 4065 is then computed to be $8.77 \pm 1.47 \times 10^{13}$ M_{sun}.

The tidal interaction perturbation between the galaxy and the cluster (P_{gc}) can now be determined using the average mass of the galaxies in the group, the average radius of the galaxies and the mass of the group (Eq. 4.2) via Eq. 2.5 , which varies along the distance from the center (R_{center}, in unit of kpc) of NGC 4065 group. The P_{gc} becomes critical (> 0.1) at 286 kpc as shown in Figure 4.12 (right).

$$M_{cluster} = 5\sigma^2 \frac{< R_{cluster} >}{G} \quad , \tag{4.2}$$

where

$MM_{cluster}$ is the mass of the group or cluster,

$R_{cluster}$ is the radius of the group or cluster, and

G is the gravitational constant.

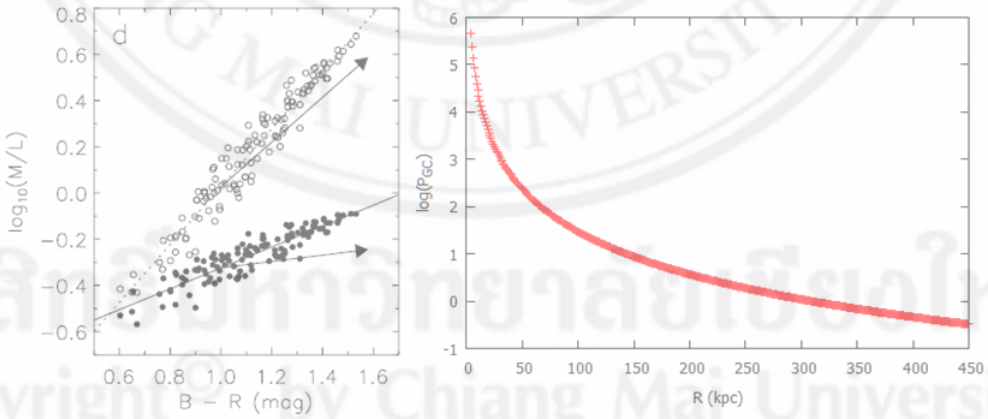

Figure 4.12: Left: The mass-to-light ratio versus $B-R$ color index. Dotted and solid lines represent the correlation in B and K band with dust extinction (arrows), respectively [Bell and de Jong, 2001], Right: The P_{gc} along the distance from the center of NGC 4065 group.

ลิขสิทธิ์มหาวิทยาลัยเชียงใหม่
Copyright© by Chiang Mai University
All rights reserved